

First-principles study on structural, mechanical and electronic properties of $\text{Li}_7\text{La}_3\text{Zr}_2\text{O}_{12}$ solid electrolyte

R Maphoto, M Masedi, P Ngoepe, R Ledwaba

Materials Modelling Centre, University of Limpopo, Private Bag x1106, Sovenga, 0727, South Africa
Email: refiloe.maphoto@ul.ac.za

Abstract

The oxide garnet $\text{Li}_7\text{La}_3\text{Zr}_2\text{O}_{12}$ (LLZO) is a promising solid electrolyte for Li-based batteries due to its high Li-ion conductivity and chemical stability with respect to Li metal anode. However, at room temperature, it crystallizes into a poorly Li-ion conductive tetragonal phase. To this end, supervalent cation doping has been an effective way to stabilize the highly conductive cubic phase and enhance the ionic conductivity of the tetragonal phase at room temperature, through the creation of lithium vacancies. Yet, the fundamental aspects regarding this supervalent substitution remain poorly understood. In this study, we have employed the first-principle calculations to offer a better understanding of the stabilization of tetragonal $\text{Li}_7\text{La}_3\text{Zr}_2\text{O}_{12}$ phases by determining the structural, mechanical, and electronic properties for high-conductivity LLZO composition. We find that the structural properties calculated are in good agreement which is within a 2% error of the experimentally measured results. The negative energy of formation for t-LLZO shows that the material is thermodynamically stable. The calculated Young's modulus is in good agreement with the experimental observations, which indicates that the material is mechanically stable. Owing to its wide electrochemical stability, the calculated band structure of t-LLZO shows that the material is a wide and indirect magnetic separator with a g-symmetry point band gap which is in good agreement with the experimental observations. Therefore, the structural, mechanical, and electronic stability of t-LLZO provides better insight about the stability of the material and this capacitates further investigations associated with ionic conductivity of the pure and supervalently doped LLZO.

1. Introduction

Li-ion batteries (LIBs) are today's most effective commercial devices for electrochemical energy storage, offering superior volumetric and gravimetric energy density compared with other battery technologies and have been widely used in power supplies such as electric vehicles, portable electronic and large-scale energy storage applications.¹ However, LIB typically contain highly flammable, volatile, and explosion accelerated organic liquid electrolytes increasing demand for safer lithium-ion batteries.¹ To this end, the conception of all-solid-state lithium ion batteries (ASSLIBs) based on solid electrolytes has been proposed and has attracted increasing attention due to its intrinsic safety, high energy density and potentially long life cycle in that it may make battery configuration more efficient, and may enable use of a metallic Li anode and high-voltage cathode.² The superior conductivity ($\sim 10^{-4}$ S.cm⁻¹) and excellent stability of the oxide garnet-type $\text{Li}_7\text{La}_3\text{Zr}_2\text{O}_{12}$ (LLZO) solid-state electrolyte has ignited significant interest for its utilization in solid-state battery technology.³ The highest lithium-ion conductivity is found with the cubic phase (space group $\text{Ia}\bar{3}\text{d}$) of the $\text{Li}_7\text{La}_3\text{Zr}_2\text{O}_{12}$ garnet.⁴ However, at room temperature, a low-energy reordering of Li-ions into the 16f, 32g (octahedral) and 8a (tetrahedral) sites of the tetragonal structure, can occur, reducing symmetry to $\text{I4}_1/\text{acd}$ (tetragonal phase). The conductivity of the tetragonal phase at room temperature is ~ 2 orders of magnitude lower than that of the cubic phase.⁵ Herein, the Density Functional Theory (DFT) was utilized to provide more details on the stability

of the tetragonal LLZO structure by determining the structural, mechanical and elastic properties as a model validation tool that will enable us to later attempt its electrochemical performance by means of supervalent doping.⁶ It is therefore important to understand the phase stability of tetragonal LLZO for further investigation and development of this promising oxide solid electrolytes.

2. Methodology

2.1 Computational procedure

The first principles approach with the Perdue-Burke-Ernzerhof (PBE)⁷ exchange-correlation functional and projector augmented wave (PAW)⁸ pseudo-potentials within the Generalized Gradient Approximation (GGA) as implemented in the Vienna ab initio Simulation Package (VASP)⁹ was employed. A $5 \times 5 \times 5$ Monkhorst-pack grid for k-point sampling, and a cut-off energy of 500eV for the structure were utilized. The self-consistency convergence criterion for the energy was set to 10^{-5} eV, and geometry relaxation was considered converged when all forces were less than $0.01\text{eV}/\text{\AA}$ with maximum stress of 0.02 GPa. For better calculations of the mechanical and electronic properties, the same above mentioned k-mesh point and cut-off energy were used. The 8-formula unit ($\text{Li}_7\text{La}_3\text{Zr}_2\text{O}_{12}$) conventional unit cell, with tetragonal symmetry group $\text{I4}_1/\text{acd}$, for lattice constant calculations was used. The structure was fully optimized, relaxing the lattice parameters and ions.

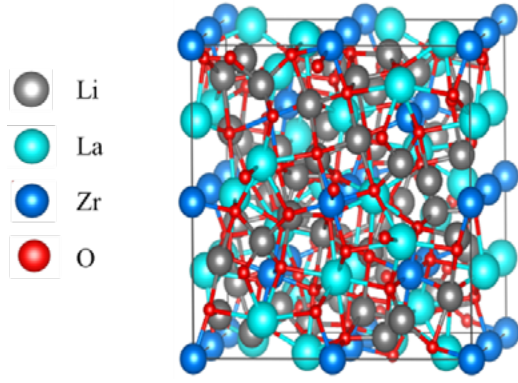


Figure 1: Crystal structure of garnet-type tetragonal $\text{Li}_7\text{La}_3\text{Zr}_2\text{O}_{12}$ (LLZO) with Li, La, Zr, and O ions shown in grey, turquoise, blue, and red, respectively

3. Results and discussion

3.1 Structural properties

The optimized tetragonal (with space group $I4_1/acd$) LLZO crystal structure is shown in figure 1. Table 1 indicates that lattice parameters found for t-LLZO unit cell are $a=b=13.12\text{\AA}$, and $c=12.67\text{\AA}$, which are consistent with the reported experimental values of $a=b=13.134\text{\AA}$, and $c=12.663\text{\AA}$.¹⁰ The heat of formation is calculated using GGA approximation. The heat of formation for t-LLZO is -6511.01kJ/mol , which indicates that the structure is thermodynamically stable. Also note that the calculated volumes for t-LLZO (2203\AA^3) compares well to the experimental value 2185\AA^3 ¹⁰ which is within a 0.824% error.

Table 1: Calculated lattice constants (\AA), energy of formation ΔH_f (kJ/mol), and volume V (\AA^3) of t-LLZO compared with other experimental results

	Tetragonal $\text{Li}_7\text{La}_3\text{Zr}_2\text{O}_{12}$	
	This work	Experimental
Lattice constant (\AA)	$a=b=13.12$ $c=12.66$	$a=b=13.13$ $c=12.66$
Energy of formation ΔH_f (kJ/mol)	-6511.01	-
Volume V (\AA^3)	2203	2185

3.2 Mechanical stability

The elastic constants are calculated to predict the mechanical stability of the materials. The elastic coefficients describe the crystal's mechanical and dynamic behaviour, and show how the structure deforms under pressure and then returns to its initial shape, and these coefficients are calculated in order to predict mechanical stability. Table 2 below shows elastic constants (C_{11} , C_{12} , C_{13} , C_{16} , C_{33} , C_{44} and C_{66}) values calculated using GGA approximation. It is clear that the elastic constants C_{ij} of t-LLZO are all positive and greater than zero, which is content with the stability conditions. Furthermore, t-LLZO is elastically stable since the elastic constants satisfy the criteria given below. Thus, the elastic stability of t-LLZO is concluded using the results obtained from Table 2 below and evaluated using the criteria below:¹¹

$$C_{11} > |C_{12}|,$$

$$2C_{13}^2 < C_{33}(C_{11} + C_{12}), \quad (1)$$

$$C_{44} > 0, 2C_{16}^2 < C_{66}(C_{11} - C_{12}).$$

$$C_{11} > 0, C_{12} > 0, C_{13} > 0, C_{16} > 0, C_{33} > 0, C_{44} > 0 \text{ and } C_{66} > 0$$

Table 2: Calculated elastic constants (C_{11} , C_{12} , C_{13} , C_{16} , C_{33} , C_{44} and C_{66}) of t-LLZO using GGA approximation

	Tetragonal $\text{Li}_7\text{La}_3\text{Zr}_2\text{O}_{12}$	
	t-LLZO	Experimental ¹²
C_{11}	177.69	169.80
C_{12}	85.46	63.90
C_{13}	80.42	-
C_{16}	1.91	-
C_{33}	205.05	-
C_{44}	76.51	69.80
C_{66}	71.27	-

According to the Hill approximations, the bulk modulus (B) and Shear modulus (G) can be obtained from the values of elastic coefficients (C_{11} , C_{12} , C_{13} , C_{16} , C_{33} , C_{44} and C_{66}). It is also possible to calculate the values of Young's modulus (E) and Poisson ratio using the following formula:¹³

$$B = \frac{C_{11} + 2C_{12}}{3} \quad (2)$$

$$G = \frac{\left[\frac{C_{11} - C_{12} + 3C_{44}}{5}\right] + \left[\frac{5C_{44}(C_{11} - C_{12})}{[4C_{44} + 3(C_{11} - C_{12})]}\right]}{2} \quad (3)$$

$$E = \frac{9BG}{3B+G} \quad (4)$$

$$\nu = \frac{3B-E}{6B} \quad (5)$$

The Young's modulus is a measure of the stiffness of a solid material, whenever the Young's modulus is high (100-200 GPa), the crystal has greater strength and hardness. Comparing the calculated values from Table 3 below and the values obtained from other works (Table 3), the reason for the small difference between them is due to the difference between the method used and approximation. However, although GGA tend to undermine elastic constants, the approximation is an excellent choice for studying elastic properties of solid electrolytes, because in comparison with experimental values, it reproduces high accuracy elastic constant results. The Shear modulus (G) demonstrates the strength of crystal to suppress lithium dendrite formation, which in this case it is stiff enough. So the ratio of the bulk modulus to the Shear modulus can be used to present an evaluation of the softness or brittleness of the material¹⁴

$$\frac{B}{G} > 1.75 \text{ implies that the material is ductile}$$

$$\frac{B}{G} < 1.75 \text{ implies that the material is brittle}$$

The calculated Pugh ratio B/G for t-LLZO indicates that the material is brittle, which is in agreement with the data from other works, and the Poisson's ($\nu = 0.258$) ratio means that the material is predominantly ionic, hence it can be used in solid state Li batteries.

Table 3: Calculated Bulk (B), Shear (G) and Young modulus (E), and Pugh ratio (B/G) modulus of t-LLZO using GGA approximation

	Tetragonal $\text{Li}_7\text{La}_3\text{Zr}_2\text{O}_{12}$		
	This work	Experimental ¹²	Other ¹³
Bulk modulus B (GPa)	112.23	99.20	111.42
Shear modulus G (GPa)	64.84	62.50	64.98
Young modulus E (GPa)	163.51	154.90	163.11
Pugh ratio B/G	1.73	1.59	1.71
Poisson's ratio ν	0.26	0.24	0.26

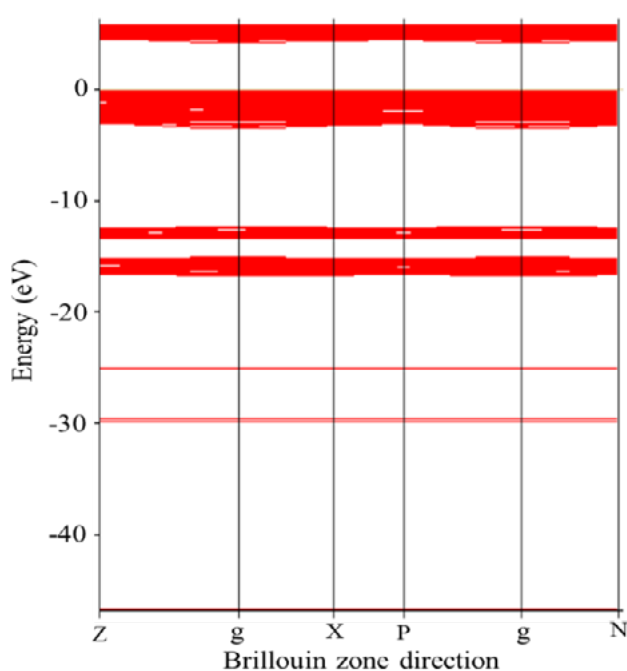
3.3 Electronic properties

3.3.1. Band structure curves.

In the curves of the band structure in Figure 2, the energy function is plotted in the first Brillouin zone versus the energy (eV). From this diagram, some important information on the crystal-electronic nature of being metal or non-metal can be predicted. In Figure 2 is the t-LLZO band structure diagram using GGA. The distance between the states at the maximum valence band (VBM) and the minimum conductive band (CBM) is determined by the electronic band gap. As a result, according to the below plotted band structure curves, t-LLZO is an insulator with a large band gap of 4.33 eV located at the g point of the Brillouin zone. The band gap is in good agreement with the experimental data which indicate that a wide electrochemical window is an intrinsic property of LLZO, facilitating its use in next-generation batteries.

3.4 Density of States

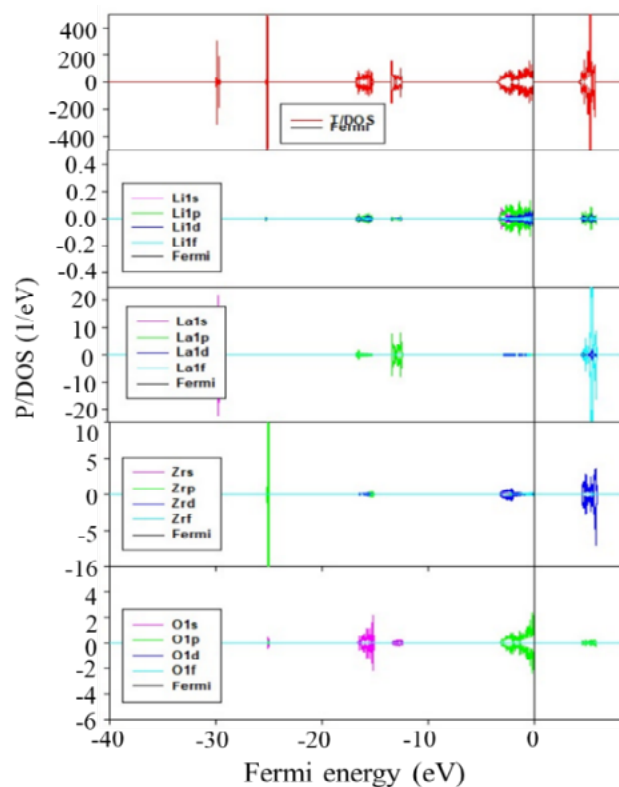
Density of states describes the probability of electron distribution in the energy spectrum. The total density of state calculations using GGA approximations for $\text{Li}_7\text{La}_3\text{Zr}_2\text{O}_{12}$ in tetragonal solid electrolyte phase at equilibrium pressure is shown in Figure 3 below, in which Fermi energy is chosen as a zero point of reference. Density of states calculations and band structure calculations exhibit significant similarities, As shown in figure 3


Figure 2: Band structure for t-LLZO solid electrolyte at equilibrium pressure using GGA approximations

below, the lower valence band (LVB) in the range of -18 to -12 eV, is formed by Li-2p, La-4p, Zr-5d, and O-2s orbitals. The upper valence band (UVB) in the range of -5 to 0 eV, which is formed by Li-2p, Zr-4f and O-2p orbitals, can be shown to be the result of the hybridization of the valence band. Lastly, the last region is the conduction band (CB) and the edge of the conduction band, as shown in figure 3 below, which is formed by the atoms La and Zr of the orbitals 4f and 5d respectively. There is a large band gap of 4.33 eV in the 5d orbital of the Zr atom, indicating that tetragonal $\text{Li}_7\text{La}_3\text{Zr}_2\text{O}_{12}$ structure is an insulator. Also, the large band gap implies that t-LLZO has a large electrochemical window. As such, tetragonal $\text{Li}_7\text{La}_3\text{Zr}_2\text{O}_{12}$ structure in a battery will prevent electronic leakage.

Conclusion

In the present study, we have performed detailed first principles calculations investigating the structural, mechanical and electronic properties of tetragonal LLZO. The t-LLZO structure was fully optimized in order to precisely reproduce reported lattice parameters. The heat of formation was found to be negative which indicated a good thermodynamic stability of the material. The elastic constants (C_{ij}) of t-LLZO satisfy the mechanical stability


Figure 3: Density of state for t-LLZO solid electrolyte at equilibrium pressure using GGA approximations

criteria. Moreover, the calculated Poisson's ratio shows that the t-LLZO is brittle and ionic, encouraging its use in the next-generation Li-ion batteries. The electronic energy band structure and DOS were found to be in good agreement suggesting that t-LLZO is a magnetic separator with a wide band gap of ~ 4.33 eV, which ensures a sufficiently wide electrochemical window for all-solid-state lithium batteries. Our analysis suggests that tetragonal LLZO is stable structurally, mechanically and electronically, paving the way for further improvement of the ionic conductivity through supervalent doping.

Acknowledgement

Financial support from the National Research Foundation (NRF) Thuthuka (Grant Unique Number: 121850) is acknowledged. This work was performed using the computational facilities of the Centre for High Performance Computing (CHPC), Cape Town and Materials Modelling Centre at University of Limpopo, in South Africa.

References

- Nitta N, Wu F, Lee J T, and Yushin G, 2015. Li-ion battery materials: present and future. *Materials today* 18, 252-264.
- Duan H, Zheng H, Zhou Y, Xu B and Liu H, 2018. Stability of garnet-type Li ion conductors: An overview. *Solid State Ionics* 318, 45-53.
- Kim A, Woo S, Kang M, Park H, and Kang B, 2020. Research progresses of garnet-type solid electrolytes for developing all-solid-state Li batteries. *Frontiers in Chemistry*, 8, 468.
- Murugan R, Thangadurai V and Weppner W, 2007. Fast lithium ion conduction in garnet-type $\text{Li}_7\text{La}_3\text{Zr}_2\text{O}_{12}$. *Angewandte Chemie International Edition*, 46, 7778-7781.
- Buschmann H *et.al.* 2011. Structure and dynamics of the fast lithium ion conductor " $\text{Li}_7\text{La}_3\text{Zr}_2\text{O}_{12}$ ". *Physical Chemistry Chemical Physics*, 13, 19378-19392.
- Bonilla M R, Garcia-Daza F A, Carrasco J and Akhmatkaya E, 2019. Exploring Li-ion conductivity in cubic, tetragonal and mixed-phase Al-substituted $\text{Li}_7\text{La}_3\text{Zr}_2\text{O}_{12}$ using atomistic simulations and effective medium theory. *Acta Materialia*, 175, 426-435.
- Perdew J P and Wang Y, 1992. Pair-distribution function and its coupling-constant average for the spin-polarized electron gas. *Physical Review B*, 46, 12947.
- Perdew J P, Burke K and Ernzerhof M, 1996. Generalized gradient approximation made simple. *Physical review letters*, 77, 3865.
- Kresse G and Furthmüller J, 1996. Efficient Iterative Schemes for ab Initio Total-Energy Calculations Using a Plane-Wave Basis Set. *Physical Review B*, 54, 11169-11186.
- Awaka J, Kijim N, Hayakawa H and J. Akimoto J, 2009. Synthesis and structure analysis of tetragonal $\text{Li}_7\text{La}_3\text{Zr}_2\text{O}_{12}$ with the garnet-related type structure. *Journal of solid state chemistry*, 182, 2046-2052.
- Mouhat F and Coudert F X, 2014. Necessary and sufficient elastic stability conditions in various crystal systems. *Physical review B*, 90, 224104.
- Yu S, Schmidt R D, Garcia-Mendez R, Herbert E, Dudney N J, Wolfenstine J B, Sakamoto J and Siegel D J, 2016. Elastic properties of the solid electrolyte $\text{Li}_7\text{La}_3\text{Zr}_2\text{O}_{12}$ (LLZO). *Chemistry of Materials*, 28, 197-206.
- Hill R, 1952. The elastic behaviour of a crystalline aggregate. *Proceedings of the Physical Society. Section A*, 65, 349.
- Pugh S, 1954. XCII. Relations between the elastic moduli and the plastic properties of polycrystalline pure metals. *The London, Edinburgh, and Dublin Philosophical Magazine and Journal of Science*, 45, 823-843.